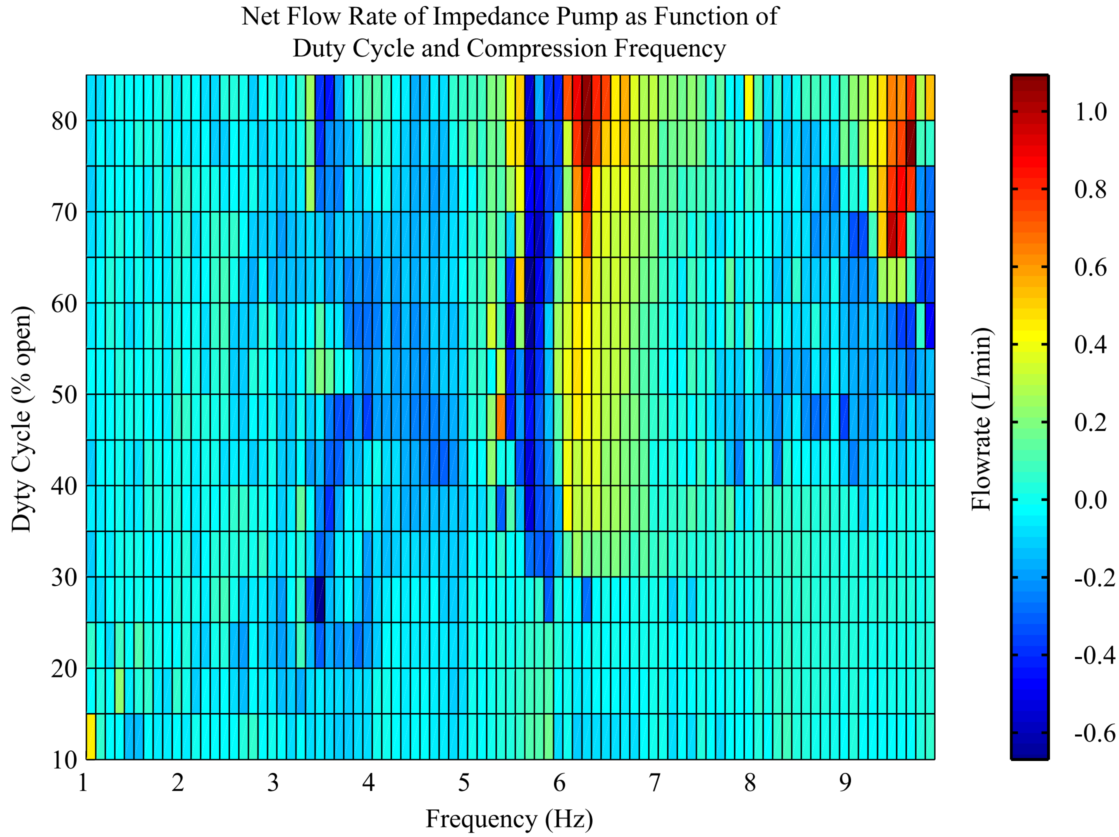

Figure 3.23: The net flow rate of the impedance pump as a function of duty cycle and compression frequency.

physically obstructed for different amounts of time and the pressure wave interaction on the tube is modified because the pressure waves can reflect off of the compression site for different amounts of time. For this configuration, the duty cycle only affects the magnitude of the net flow but not the direction or frequency response. This is caused by the obstruction to flow. In another configuration with less attenuation, the duty cycle may have more effect because the amplitude of the pressure wave will be greater when it returns to the pincher location.

3.3.7 Bulk Flow Efficiency

The efficiency of the impedance pump system may be separated into three parts: the electromechanical efficiency of the compression mechanism, the efficiency in the

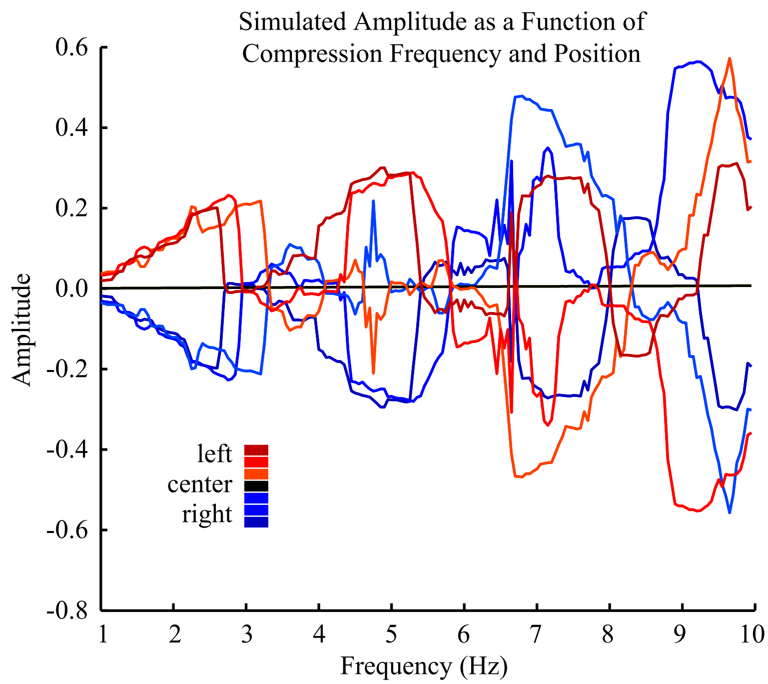

Figure 4.2: Simulation of wave amplitude difference as a function of compression frequency and position.

the summed wave amplitude at the ends of the line represent a value proportional to the pressure head of a similar pump. Once an equilibrium is reach a mean value of the amplitude difference can be taken for varying compression frequencies.

The model was implemented using C++ code. We find similar results to those of the experiments: the frequency response in the time-averaged amplitude difference across the length of the model shifts with the position of compression and is symmetric about the center (figure 4.2); and the frequency response increases linearly with the wave speed (figure 4.3). Additional results from the simulation show that the pulse width greatly affects the amplitude of the difference across the length of the pump (figure 4.4). The reflectance coefficient induces a similar behavior. As the reflectance coefficient increases, so does the amplitude difference across the length. As the reflectance coefficient goes to zero, no net difference is found across the pump (figure 4.5).

A comparison can be made between the experimental results and the simulation

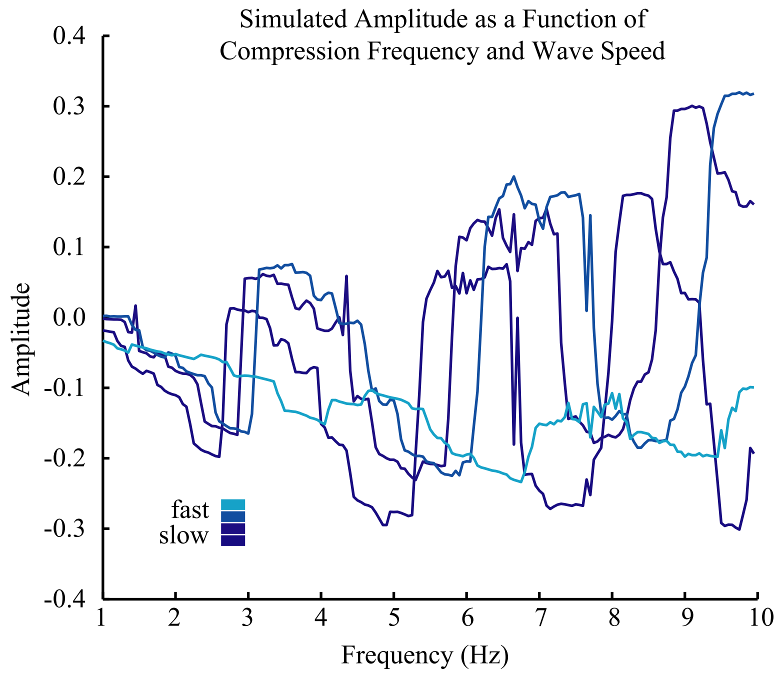

Figure 4.3: Simulation of wave amplitude difference as a function of compression frequency and wave speed.

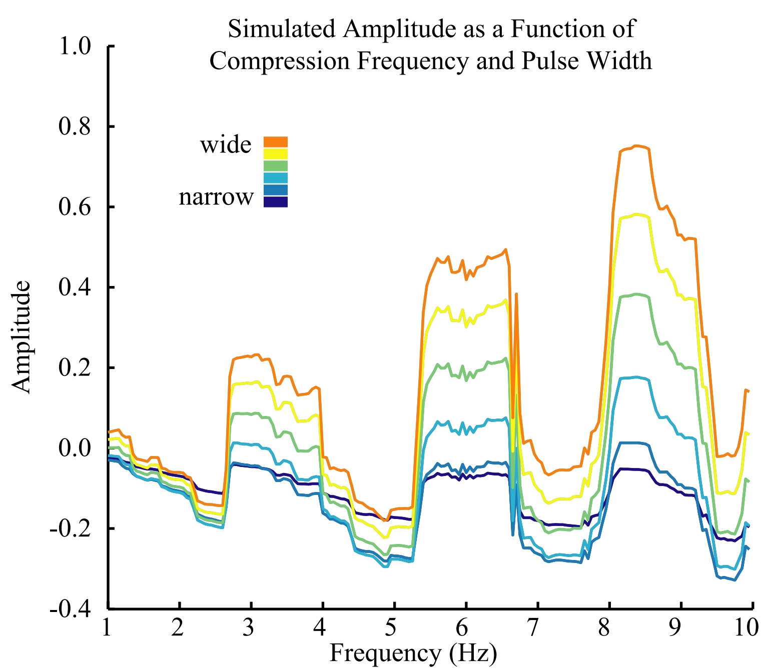

Figure 4.4: Simulation of wave amplitude difference as a function of compression frequency and pulse width.

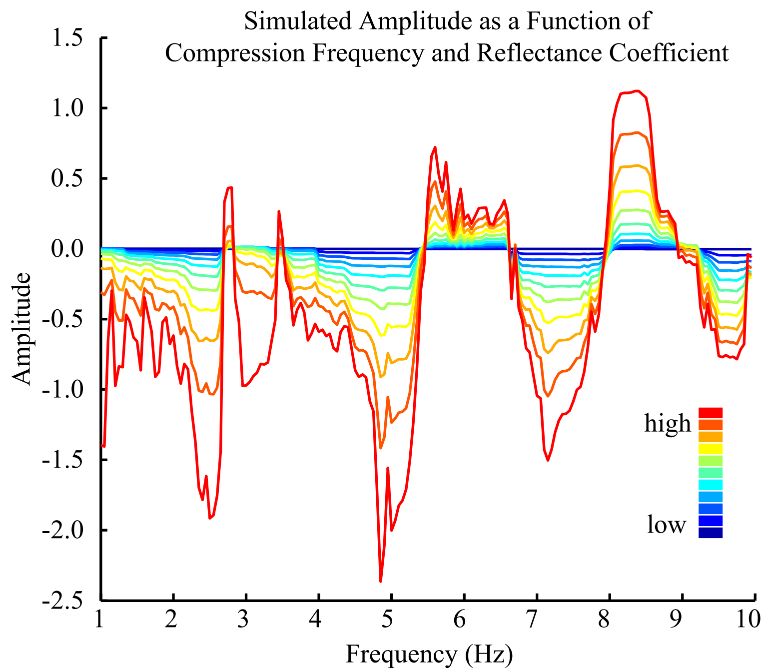

Figure 4.5: Simulation of wave amplitude difference as a function of compression frequency and reflectance coefficient.

using parameters in the range known to be accurate for a specific experiment (table 4.4). Many of the parameters are easily applied from the experiments. To maintain convention used in the experiments, duty cycle is the fraction of the compression period that the pinchers are not in contact with the tube. As was discussed in section 3.2.1, the pinchers only remain in contact with the tube during the compression and not retraction when the motorized compression mechanism is used and the duty cycle had been adjusted accordingly. The parameters that remain unknown are the amplitude of the pressure wave, the waveform including its shape and width, the amplitude decay constant, and the reflectance coefficient. If we do not concern ourselves with the scale of the simulated results, but instead we worry just about the shape, we can safely select the initial wave amplitude, pulse width, and reflectance coefficient without affecting the overall shape. This leaves the shape of the waveform and the amplitude decay constant up to interpretation. The shape chosen was a simple Gaussian loosely based on the ultrasound images of the tube wall. The decay constant was

Figure B.1: Photograph of a stereolithography model of the rotary viscous pump.

shaft that was connected to an external brushless motor. The pump was incorporated into a test loop consisting of two pressure transducers located at the inlet and outlet of the pump, a transonic flow transducer, a reservoir of fluid, and an adjustable ball valve. Sections of the loop were made from Tygon 3603 tubing and connected with quick release connectors.

Two sets of data were collected for each case explored. In the first test, the ball valve was left completely open while the angular velocity of the shaft was adjusted by steps of approximately 1000 rpm. Ten samples were taken for each data point over ten seconds. Measurements were taken through a National Instruments DAQ board and recorded using LabVIEW. Data collected included the inlet pressure, outlet pressure, flow rate, and the power consumption of the motor.

In the second test, the angular speed of the shaft was set to the constant rate of 7650 rpm. In this case, however, the opening of the ball valve was adjusted in steps of 15 deg to modify the resistance of the loop. The data were collected in the same manner as the first test.

B.3 Stereolithography Results

A variety of design parameters were modified and tested. To begin, we tested the performance of our initial design with both water and 31% by volume glycerol solution corresponding to a viscosity of 3.082 g/cm-sec, similar to that of blood (figure B.2).

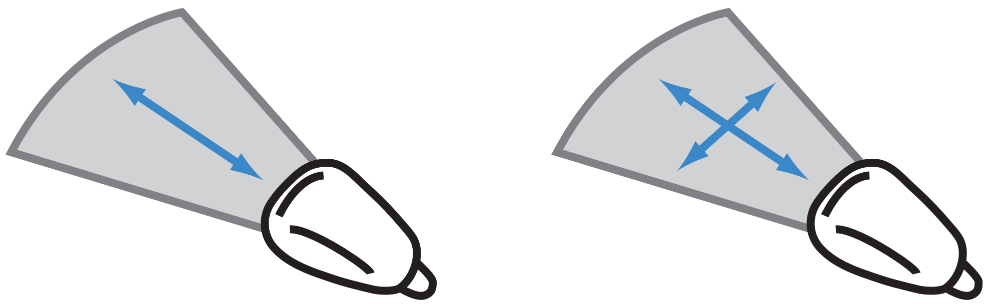

(a) ultrasound Doppler (b) digital ultrasound speckle image velocimetry

Figure C.1: Ultrasound Doppler and DUSIV velocity directions

C.3 Digital Speckle Image Velocimetry

Digital ultrasound speckle image velocimetry (DUSIV), a hybrid between ultrasound imaging and digital particle image velocimetry, is a technique for obtaining two-dimensional flow field data. The ultrasound can be used to take images of a flow through an optically opaque body. By seeding the flow with particles that reflect ultrasound waves, one can obtain images similar to those used for DPIV (figure C.1(b)).

There remain a number of critical differences in ultrasound images that distinguish them from DPIV:

- The images acquired by ultrasound are captured in polar coordinates. This results in non-uniform resolution of the image when transformed into Cartesian coordinates.

- The individual particles are not resolved in the ultrasound images. Instead, regions in the flow where the density of particles is higher collectively reflect the ultrasound and are realized as speckles in the image.

- The pixels of the image are captured sequentially. This means that the time at which one pixel of the image was taken is not the same as the time another pixel was taken. However, the time step between any pixel in one frame and the same pixel in another frame should be constant for all pixels.

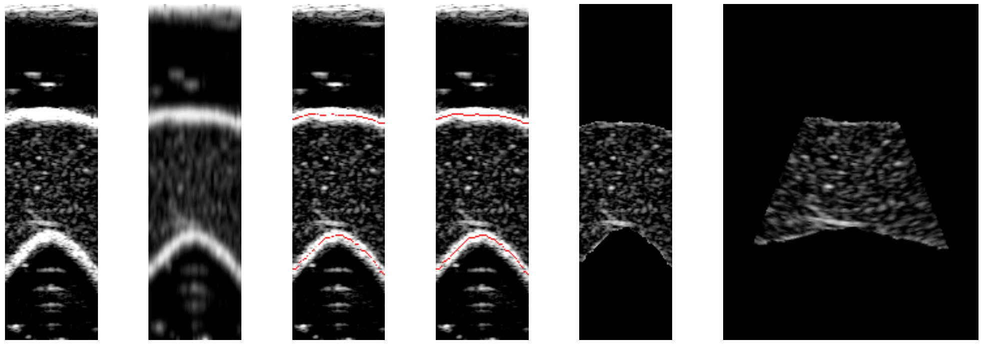

(a) (b) (c) (d) (e) (f)

Figure D.1: Processing steps of the edge-detection software (left to right: original image, box-blurred, maxima points located, maxima points linked into a chain, original image masked, coordinates converted from polar to Cartesian)

- The process is repeated by successively blurring the image until there are only two chains that match the minimum length criteria. Those chains represent the edges of the tube.
- The original image is then masked on the walls and outside the tube based on the edge locations found (figure D.1(e)).
- The masked image is transformed from polar coordinates to Cartesian coordinates for use with the DUSIV software (figure D.1(f)).

D.2 Using the Program

To compile the program, one must have a C compiler, glib 1.2, and a few other C libraries. Use the command:

```
prompt: gcc -o edgefind edgefind.c `glib-config --cflags --libs` -lm
```

Once compiled the program can be run in a shell by typing:

```
prompt: edgefind < input.pgm > output.ppm
```

The program will use the file, `input.pgm` as its input and `output.ppm` as the output file. In order to perform this task on many bitmap files, one can use the